Revealing Time-Varying Joint Impedance With Kernel-Based Regression and Nonparametric Decomposition

van de Ruit, Mark; Cavallo, Gaia; Lataire, John; Van Der Helm, Frans C.t.; Mugge, Winfred ; van Wingerden, Jan-Willem; Schouten, Alfred C.

Published in:
IEEE transactions on control systems technology : a publication of the IEEE Control Systems Society.

DOI:
10.1109/TCST.2018.2881664

Publication date:
2020

Document Version:
Accepted author manuscript

Revealing time-varying joint impedance with kernel-based regression and non-parametric decomposition

Mark van de Ruit, Gaia Cavallo, *Student Member, IEEE*, John Lataire, *Member, IEEE*, Frans C. T. van der Helm, Winfred Mugge, Jan-Willem van Wingerden, and Alfred C. Schouten

***Abstract*—During movements humans continuously regulate their joint impedance to minimize control effort and optimize performance. Joint impedance describes the relationship between a joint's position and torque acting around the joint. Joint impedance varies with joint angle and muscle activation, and differs from trial-to-trial due to inherent variability in the human control system. In this study a dedicated time-varying system identification framework is developed involving a parametric, kernel-based regression, and non-parametric, 'skirt decomposition', system identification method to monitor the time-varying joint impedance during a force task. Identification was performed on single trials and the estimators included little a prior assumptions regarding the underlying time-varying joint mechanics. During the experiments, six (human) participants used flexion of the wrist to apply a slow sinusoidal torque to the handle of a robotic manipulator, while receiving small position perturbations. Both methods revealed that the sinusoidal change in joint torque by activation of the wrist flexor muscles resulted in a sinusoidal time-varying joint stiffness and resonance frequency. A 3rd-order differential equation allowed the parametric kernel-based estimator to explain on average 76% of the variance (range 52-90%). The non-parametric skirt decomposition method could also explain ~76% of the variance (range 51-89%). This study presents a novel framework for identification of time-varying joint impedance making use of linear time-varying models based on a single trial of data.**

***Index Terms*—Joint impedance, System identification, Time-varying systems, human motor control**

This research was funded by the European Research Council under the European Union's Seventh Framework Programme (FP/2007-2013) ERC Grant Agreement n. 291339, project 4DEEG: A new tool to investigate the spatial and temporal activity patterns in the brain. John Lataire is supported in part by the Flemish Government (Methusalem) and the Belgian Government through the Inter university Poles of Attraction (DYSCO) Program.

Mark van de Ruit, Frans CT. Van der Helm, Winfred Mugge and Alfred C. Schouten are with the Laboratory for Neuromuscular control, Department of Biomechanical Engineering, Delft University of Technology, Mekelweg 2, 2628CD, Delft, The Netherlands (e-mail: m.l.vanderuit-1@tudelft.nl; f.c.t.vanderhelm@tudelft.nl; w.mugge@tudelft.nl; a.c.schouten@tudelft.nl)

John Lataire and Gaia Cavallo are with the Department of Electrical Engineering, Vrije Universiteit Brussel, 1050 Brussels, Belgium (e-mail: John.Lataire@vub.be; gaia.cavallo@vub.be)

Jan-Willem van Wingerden is with the Delft Center for Systems and Control, Delft University of Technology, Mekelweg 2, 2628CD, Delft, The Netherlands (e-mail: j.w.vanwingerden@tudelft.nl)

I. Introduction

HUMANS are able to perform skillful movements despite challenging environmental circumstances or the presence of external disturbances. Information provided by the body's internal sensors (proprioceptors) and actions executed by the body's actuators (muscles) are used to achieve this. Hereby, humans can adapt the dynamics of their joints by regulating their intrinsic and reflexive joint properties [1]. Ensuring adequate task performance at all times, the controller of the human bodyFig, i.e. the central nervous system, follows the principles of optimality and control effort minimization [2].

System identification (SI) can be used to quantify properties of the human joints during posture and movement. For example, joint impedance, describing the joint's resistance to external disturbances, may be determined by relating joint position and torques in response to a mechanical perturbation [1, 3-9]. However, joint impedance is affected by many physiological and mechanical factors like muscular fatigue [10], joint angle and muscle activation level [7]. Therefore, time-invariant SI techniques are only applicable when the system remains in a fixed operation point, i.e. there are only small changes in joint angle or muscle activation. When this is not the case, time-varying SI techniques allow to study changing joint impedance across time, e.g. as a function of joint angle or muscle activation level.

There are many SI techniques for time-varying systems that have been employed to investigate various engineering challenges like a metal's electrical impedance changing as a result of pit corrosion [11], varying mechanical loads to bridges and buildings [12, 13] or aeroelastic flutter during flight [14]. In all cases, the system dynamics can be described using a model which is either parametric or non-parametric in its dynamics and time variation. Both parametric and non-parametric models may be used to obtain a time-varying frequency response function (TV-FRF) that provides a description of the time-varying system dynamics. For parametric models, systems are typically described by using differential equations with time-varying coefficients. The differential equations can be expressed in the time- or frequency domain to define the assumed model structure [15, 16]. The time-varying coefficients are expressed using time-dependent basis functions, which may be e.g. wavelets, sines

and cosines or Legendre polynomials. Alternatively, time-varying autoregressive moving average (ARMA) models have been successfully applied to estimate TV-FRFs [17].

An example of a non-parametric SI tool to provide a time-dependent spectral representation of a non-stationary signal is the short-time Fourier transform (STFT) [18]. In the STFT, a linear representation of the signals is constructed within a short, fixed length time window. Subsequently the TV-FRF is created by sliding the window over time. Other non-parametric tools to analyze non-stationary signals include wavelets and Cohen's class of distributions [18]. These methods have been successfully used to extract time-varying system properties [e.g. 19, 20]. The advantage of non-parametric models over parametric models is that they require very little to no a priori assumptions on the model structure and order [21].

Both parametric and non-parametric models have been used to describe time-varying joint impedance [20-29]. A 2nd-order mass-spring-damper system is often assumed to represent joint dynamics. Therefore, a 2nd-order parametric model based on linear differential equations has often been used to describe joint properties [22-24]. For example, in [25] a parametric ARMA model is used to describe elbow stiffness during cyclic movements. Non-parametric models have also been used to describe joint properties in both the time [4, 26-30] and frequency domain [31].

A challenge in estimating time-varying joint properties is the poor signal-to-noise (SNR) ratios of human physiological and mechanical signals which typically ranges between -20 and 30 dB [32]. These noise levels are (too) high for accurate identification of joint properties. Therefore, a good model of joint properties can only be obtained by averaging repetitive measurements of the same time-varying behavior before the model is estimated, a process called ensemble averaging. With ensemble averaging the SNR is improved as the noise is typically random and reduced by the averaging. When studying time-varying behaviors, there are various downsides to the need for ensemble averaging. Firstly, it may conceal important adaptations in motor control and interesting trial-to-trial variability [33, 34] of the joint properties and motor performance. Secondly, as lots of data is required while the experimental time is limited participants may suffer from muscular fatigue and lapses in attention that will affect the behavior. Therefore there is an increased need for SI methods that allow for the estimation of joint properties based on a single trial of data, the feasibility of which has been demonstrated previously [17, 35, 36].

The aim of this paper is to validate one parametric and one non-parametric linear time-varying (LTV) SI technique for identifying time-varying joint impedance of the human wrist. This will be done based on single trial data recorded from a postural task during which participants exert a time-varying flexion torque. The presented methods provide a novel framework for LTV methods to assess time-varying human joint properties with limited experimental constraints.

In section II and III the SI methods employed to study joint impedance are outlined. Section IV describes a simulation study, used to demonstrate validity of the presented SI methods when identifying a known time-varying joint impedance. Following the simulation study, an experimental study was performed which is described in section V. Finally, in section VI the results are interpreted and discussed.

II. Skirt Decomposition Method

In this section, we introduce a non-parametric estimator to identify continuous-time linear time-varying systems. The estimator allows to identify an unknown time-varying system based on the response to a periodic multisine perturbation signal [37].

A. Background

The behavior of a time-varying system G is considered linear with respect to its arbitrary input $u(t)$ and response output $y(t)$. The latter can be computed as:

$$y(t) = G\{u(t)\} \equiv \int_{-\infty}^{\infty} g(t,\tau)u(\tau)d\tau, \tag{1}$$

where $g(t,\tau)$ is the time-varying impulse response function of G. This means that $g(t,\tau)$ is the response of the system at time t to an impulse applied at time τ. The Fourier transform of the time-varying impulse response function defines the system function or time-varying FRF $G(j\omega,t)$ [38]:

$$G(j\omega,t) = \int_{0}^{\infty} g(t,t-\tau)e^{-j\omega\tau}d\tau, \tag{2}$$

The system function $G(j\omega,t)$ relates the Fourier transform of the perturbation signal $U(j\omega)$ to the output signal $y(t)$ as

$$y(t) = \frac{1}{2\pi}\int_{-\infty}^{\infty} G(j\omega,t)U(j\omega)e^{j\omega t}d\omega, \tag{3}$$

For convenience of the identification procedure elaborated further down, we write the system function $G(j\omega,t)$ as a series expansion.

$$G(j\omega,t) = \sum_{p=0}^{\infty} G_p(j\omega)b_p(t) \tag{4}$$

with $\{b_p(t)\}_{p=0}^{\infty}$ representing a complete set of basis functions. These basis function are used to represent the time variation across a series of LTI systems G_p. By inserting (4) into (3), the system behavior is described by

$$y(t) = \sum_{p=0}^{\infty} G_p\{u(t)\}b_p(t), \qquad \forall t \in [0,T] \tag{5}$$

where $G_p\{u(t)\}$ is the response of an LTI system G_p to an input $u(t)$ applied during a time window of length T.

B. Identification procedure

The goal is to extract a non-parametric estimate of the FRFs of the LTI systems $G_p(j\omega)$ for a given (or chosen) set of basis functions. The strategy consists of applying a sparse multisine as excitation signal. The multisine perturbation is defined as:

$$u(t) = \sum_{k_e \in \mathbb{K}_{exc}} A_{k_e}\cos(\omega_{k_e}t + \phi_{k_e}) \tag{6}$$

Thus, the multisine signal is a sum of cosines, with

- angular frequencies $\omega_{k_e} = 2\pi k_e/T_{ms}$, where T_{ms} is

the length (in s) of the multisine signal,

- $\mathbb{K}_{\text{exc}} \subset \mathbb{N}$ a sparse set of excited frequency bins, chosen sufficiently separated to ensure the identifiability of the model (as elaborated in [37]).
- amplitudes A_{k_e}, which, in concordance with $\mathbb{K}_{\text{exc}}$, determine the spectral content of the perturbation.
- phases ϕ_{k_e}, which are chosen randomly, uniformly distributed in $[0,2\pi[$.

Considering that a multisine is used as an excitation signal, the system equation (5) can be rewritten in terms of the discrete Fourier transforms (DFTs) of the perturbation signal, output signal and basis functions (denoted $U(k)$, $Y(k)$ and $B_p(k)$ respectively) as:

$$Y(k) = \frac{1}{N}\sum_{p=0}^{N_\text{p}} \sum_{k_\text{e}\in\mathbb{K}_\text{exc}} G_p(j\omega_{k_\text{e}})U(k_\text{e})B_p(k-k_e) \ldots + T_Y(j\omega_k) \quad (7)$$

where the sum in (5) has been truncated to the first N_p terms, where N_p is the order of the time variation. $T_Y(j\omega_k)$ captures transient effects, which are due to the difference between the initial and end conditions of the system. It is assumed that the applied input DFT $U(k)$ is known, and that measurements $Y_m(k)$ of the output DFT spectrum are available, corrupted by an additive output noise $V(k)$:

$$Y_m(k) = Y(k) + V(k) \quad (8)$$

In (7), the output DFT spectrum $Y(k)$ of the system model is linear in the FRFs $G_p(j\omega_{k_\text{e}})$, for $p = 0, \ldots, N_\text{p}$ and $k_\text{e} \in \mathbb{K}_\text{exc}$. Thus, these FRFs can be extracted from the measured output by a linear least squares algorithm. This results in a maximum likelihood estimator under some weak assumptions (Assumption 7 in [37]) on the measurement noise $V(k)$ (which should be uncorrelated over the frequencies) and for an implementation in a sliding frequency domain window, as explained in Appendix VIII.A. Note that G_p is only estimated at a discrete set of frequencies (known as the excited frequencies of the multisine). For this reason, this estimate is called 'non-parametric'.

Sparsity of the multisine is important to obtain a well-posed problem. Namely, in (7), the number of unknowns equals $N_\text{p} \cdot N_\text{exc}$ (where N_exc is the cardinality of $\mathbb{K}_\text{exc}$, i.e. the number of excited frequencies). A necessary condition for the problem to have a unique solution is that $N_\text{p} \cdot N_\text{exc}$ is smaller than the number of data points (which equals the number of bins in the frequency band of interest). This is illustrated in Fig. 1, for $N_\text{p} = 7$. The black dots give the output spectrum $Y(k)$ in a limited frequency band, which comprises 3 excited frequencies (vertical arrows). Due to the time-varying character of the system, the output spectrum consists of skirt-shaped contributions around the excited frequencies. These 'skirts' are modelled in (7) as linear combinations of terms of the form $G_p(j\omega_{k_\text{e}})U(k_\text{e})B_p(k-k_\text{e})$. Hence the sparsity of the set of excited frequencies is important to enable distinguishing the individual terms.

Fig. 1 approximately here

III. KERNEL-BASED REGRESSION METHOD

In this section, we introduce a parametric estimator to identify continuous-time linear time-varying systems. The estimator was adopted as suggested in [39].

The system's input and output signals, $u(t)$ and $y(t)$, are assumed to satisfy a linear differential equation of the form:

$$y(t) = -\sum_{n=1}^{N_a} a_n(t)\frac{d^n y(t)}{dt^n} + \sum_{n=0}^{N_b} b_n(t)\frac{d^n u(t)}{dt^n} \quad (9)$$

Where $a_n(t)$ and $b_n(t)$ are the time-varying coefficients which are smooth functions of t. These coefficients are estimated via kernel-based regression (KBR). In essence, the estimate is defined as the following minimizer:

$$\hat{a}_n, \hat{b}_n = \underset{a_n, b_n}{\text{argmin}} \sum_{k\in\mathbb{K}_\text{int}} \frac{|E(k, a_n, b_n)|^2}{\hat{\sigma}_E^2(k, a_n, b_n)} + R(a_n, b_n) \quad (10)$$

where E is the DFT of the equation error (i.e. the difference between the left and right hand side of (9)), evaluated in $\mathbb{K}_\text{int}$, and a_n and b_n are vectorised versions of $a_n(t)$ and $b_n(t)$ in $t = 0, T_s, \ldots, (N-1)T_s$. $\mathbb{K}_\text{int}$ represents the bins of the frequency band of interest and $\hat{\sigma}_E^2$ is (an estimate of) the noise variance of E. $R(a_n, b_n)$ is a quadratic regularisation term, to impose the smoothness of the estimates. This is elaborated in more details in Appendix VIII.B, and in Lataire, et al. [39].

IV. SIMULATION STUDY

In this section, a simulation study is described to confirm the validity of the SI methods with a known time-varying stiffness.

A. Modelling human joint dynamics

A time-varying wrist stiffness was simulated using a model describing endpoint dynamics of a joint interacting with a 1 degree-of-freedom robotic manipulator. The dynamics of the joint, when only small rotations are applied, can be represented by a simple 2nd-order IBK model $H_i(s)$ together with the visco-elasticity of the interaction between manipulator and human $H_c(s)$ [1]:

$$H_i(s) = \frac{1}{Is^2 + bs + k} \quad (11)$$

$$H_c(s) = b_c s + k_c \quad (12)$$

in which s is the Laplace variable and equals $j2\pi f$ (f represents the frequency) when evaluated on the imaginary axis. $H_i(s)$ represents the intrinsic and reflexive joint dynamics where I is the limb inertia, b the joint viscosity and k the static joint stiffness. $H_c(s)$ represents the contact dynamics, a simple spring-damper system where b_c is the contact viscosity and k_c the contact stiffness.

The overall system representing the mechanical joint impedance from joint angle ($u(t)$ – and taken equivalent to

the angle of the handle of the manipulator) to joint torque ($y(t)$) is then:

$$H_{\text{wrist}}(s) = \frac{H_c(s)}{1 + H_c(s)H_i(s)} = \frac{Is^3 + (b_c b + k_c I)s^2 + (b_c k + k_c b)s + kk_c}{Is^2 + (b + b_c)s + (k + k_c)} \quad (13)$$

The system considered is shown in Fig. 2.

Fig. 2 approximately here

B. Model Implementation

The system as presented in Fig. 2 was implemented in MATLAB 2017b - Simulink 9.0 (The MathWorks, Inc., Natick, Massachusetts, United States). Output noise $v(t)$ was added as a 15 Hz low-pass filtered (2nd order Butterworth) Gaussian white noise. The amplitude of the noise was adjusted to result in a signal-to-noise ratio of the output of 10 dB, in line with previous simulation studies on joint impedances [35, 40].

C. Simulation parameters

The system, representing a human wrist joint, was simulated for 50 s (f_s = 2500 Hz), with a sinusoidally time-varying joint stiffness (k) at 0.05 Hz between ~4.7 and 6.5 Nm/rad. Limb inertia (I) and joint viscosity (b) were considered time-invariant and taken as 3 gm^2 and 0.035 Nms/rad respectively. Contact dynamics was also considered time-invariant (b_c = 10 Nms/rad, k_c = 100 Nm/rad). In total three trials were simulated, one with no noise (SNR = Inf dB) and two with both a SNR of 10 dB but different noise realizations.

D. Perturbation signal design

Random-phase multisine perturbations were used as the input signal to the simulations. Each multisine perturbation signal had a period of 10 s with excited frequencies 0.1-19.3 Hz and a spacing of 0.8 Hz between the excited frequencies. The perturbation signal was designed such that the rotation of the wrist had a root mean square (RMS) value of ≈1.1° (0.02 rad). A perturbation signal with a bandwidth limited to 20 Hz is able to reveal all relevant wrist joint dynamics [41]. The magnitude of each excited frequency was constant up to 6 Hz and decreased at higher frequencies (slope of -20 dB/decade).

E. Data Analysis

Before applying the KBR and the skirt decomposition identification algorithms the data was decimated in the frequency domain to a sampling frequency of ~ 44 Hz. Subsequently, data of the first and last 5 seconds of each trial was discarded as it was only used for initialization and did not contain a perturbation. Finally, data is only shown in the time interval [0,30] s. The estimate in the intervals [-5,0] s and [30,35] s is unreliable because of initial transient effects.

Skirt decomposition

For the skirt decomposition method, the basis functions $b_p(t)$ used in this work are the following:

$$\begin{aligned} b_0(t) &= 1 \\ b_1(t) &= 2t/T - 1 \\ b_p(t) &= \cos(\omega_{p/2} t) \qquad p > 1, p \text{ even} \\ b_p(t) &= \sin(\omega_{(p-1)/2} t) \qquad p > 1, p \text{ odd} \end{aligned} \quad (14)$$

Considering $B_p(k) = \text{DFT}\{b_p(t)\}$, the individual terms $G_p(j\omega_{k_e})U(k_e)B_p(k - k_e)$ from (7) can be recognized in Fig. 1:

- the vertical arrows (excited frequencies) are terms with $p = 0$. Since b_0 is a constant, see (14), $B_0(k - k_e)$ is only different from 0 when $k = k_e$ in (7).
- the grey full lines are terms with $p = 1$. With b_1 being a ramp, $B_1(k - k_e)$ is an (approximate) hyperbolic function, centered around the excited frequency bin k_e.
- the grey circles are terms for $p > 1$. (Co)sines have discrete Fourier transforms, which allow to capture individual bins of the output spectrum, at both sides of each excited frequency.

Since b_0 is a constant, and $b_p(t)$ for $p > 0$ is zero mean in the measured time window (T). G_0 represents the Best Linear Time Invariant (BLTI) approximation of the system, as defined in [42, 43]. (Co)sines are included as basis functions in (14) to account for the periodic nature of the imposed time variation.

The order of the time variation was set to $N_p = 7$. This is motivated by the observation that, in about six unexcited bins around the excited frequency (namely three to its left and three to its right), the output spectrum has a value which is significantly higher than the noise. By using $N_p = 7$, we have a total of six goniometric basis functions (see (14)), which allow to capture these six bins.

Kernel based regression

In this study, for the kernel based regression method, outlined in Section III, the regularisation term R uses a kernel matrix K obtained from the squared exponential kernel:

$$K(t, t') = \gamma e^{\frac{-(t-t')^2}{\sigma^2}}, \quad t, t' = 0, T_s, \dots, (N-1)T_s \quad (15)$$

in which σ determines the smoothness of the estimated time-varying coefficients. The hyperparameter γ represents the inverse of the amount of regularisation applied, defining a bias versus variance trade-off of the estimated coefficients. The hyperparameters γ and σ together determine the complexity of the estimated model.

The assumed model structure has a 3rd-order numerator and 2nd-order denominator, based on the assumed system of joint impedance (13). Therefore, the parameter N_a was chosen as 2 and N_b as 3. We define the frozen transfer function of the time-varying system as:

$$H_{\text{wrist}}(s, t^*) = \frac{b_3(t^*)s^3 + b_2(t^*)s^2 + b_1(t^*)s + b_0(t^*)}{a_2(t^*)s^2 + a_1(t^*)s + a_0(t^*)} \quad (16)$$

When evaluated in t^*, the function $H_{\text{wrist}}(s, t^*)$ is the transfer function of the LTI system, obtained by fixing the time-

varying parameters to their values at time instant t^*, i.e. $a_n(t^*)$ and $b_n(t^*)$.

The hyperparameter σ was chosen based on the periodicity of the time-varying stiffness as $\sigma \approx 20s$ in case of the presence of noise. For the noiseless case, σ was reduced to ~8 s. This increases the flexibility of the estimator and, thus, reduces the bias (this is important to show the correctness of the estimator). In addition, γ was chosen based on the variance of the data in presence of noise as the estimate was insensitive to the precise value of γ in a wide range. When no noise was present in the simulation, γ was set to 25.000.

Quality of the estimators

The quality of the estimators was determined in time domain using the variance-accounted-for (VAF). The identification was performed on a trial with output noise and validated on one trial with a different noise realization and one trial without noise. $\mathrm{VAF}_{\mathrm{self}}$, determined on the estimation data set, and $\mathrm{VAF}_{\mathrm{val}}$ determined on a validation data sets, were calculated according to:

$$\mathrm{VAF} = 1 - \frac{\mathrm{var}(y(t) - \hat{y}(t))}{\mathrm{var}(y(t))} \tag{17}$$

where $y(t)$ is the measured torque and $\hat{y}(t)$ is the simulated output based on the estimated model. In addition, true simulated joint stiffness and estimated joint stiffness, extracted as the magnitude of the FRF at the lowest frequency, were compared. For this study the difference between system function or TV-FRF (2) and frozen FRF as extracted from (9), are neglected.

F. Results

Fig. 3 presents the estimated joint stiffness as a function of time in comparison to the known true stiffness as imposed in simulation. When joint stiffness is estimated based on a trial without noise the true stiffness is closely matched for both analysis methods. Identification of the joint stiffness from a simulation trial with a SNR of 10 dB still allows extracting the sinusoidal periodicity but with a mismatch to the true stiffness. The estimate of joint stiffness by the skirt method is more affected by the presence of noise than the KBR method.

Table I shows the quantitative results using the VAF on the joint torque. Based on the VAF on the estimation data (with noise) both methods provide a good model for the data ($\mathrm{VAF}_{\mathrm{self}}$ > 96%). When validating the model VAF is still high ($\mathrm{VAF}_{\mathrm{val}}$ >94%). The KBR method achieves a higher VAF ($\mathrm{VAF}_{\mathrm{val}}$ = 96.7%) on the validation set then the skirt method ($\mathrm{VAF}_{\mathrm{val}}$ = 94.9%). Both methods provide an excellent estimate of the true FRF despite the noise as evident from the VAF on a trial without noise ($\mathrm{VAF}_{\mathrm{val}}$ > 98%). The KBR method ($\mathrm{VAF}_{\mathrm{val}}$ = 99.9%) outperforms the skirt method ($\mathrm{VAF}_{\mathrm{val}}$ = 98.2%).

Table I approximately here

Fig. 3 approximately here

V. Experimental Study

This section describes how the experimental study was performed.

A. Subjects

Six healthy participants (2 men; 33 ± 4.2 years, 4 women; 28 ± 4.1 years) with no self-reported history of neurological or orthopedic arm problems, participated in the experiment. All participants were right handed. The study was approved by the human research ethics committee (HREC) of Delft University of Technology, and all participants provided written informed consent before participating.

B. Experimental Setup

A torque-controlled wrist manipulator applied angular position perturbations to the wrist of the right arm [44]. The manipulators' handle is actuated by an electric motor (Baumuller DSM-130N) via a lever which ensures the motor axis is aligned with the axis of rotation of an average wrist. A torque sensor, consisting of strain gauges, was mounted halfway the lever to measure the torque applied by the participant. The core of the haptic controller is its velocity servo, which has a bandwidth of ~50 Hz.

Every participant was comfortably seated in front of the manipulator and asked to grab the handle with the right hand. To ensure a firm and time-invariant grip, Velcro was used to strap participants to the handle and the lower arm was immobilized. During the perturbations, the participants were asked to apply a prescribed time-varying torque. A screen in direct line of sight of the participant provided a target line, representing the torque that had to be exerted, and a cursor, that was indicative for the exerted torque (0.6 Hz low-pass filtered). Participants were instructed to trace the target line with the cursor throughout each trial. Fig. 4 provides a schematic of the experimental setup. During all trials, the torque on the handle and position of the handle were measured, sampled at 2500 Hz and stored.

Fig. 4 approximately here

C. Measurement Protocol

The participants completed 12 trials, 6 trials each for two different tasks. Before the trials, the maximum voluntary torque (MVT) was determined. The first task required the voluntary modulation of flexion torque. Participants had to vary their exerted flexion torque between 5-20% MVT according to a sinusoidal pattern (with a frequency of 0.05 Hz). Participants were instructed to track a target line presented on the screen while ignoring the continuous multisine angular perturbation on the handle of the manipulator. The torque variations due to the perturbation were much smaller than the requested voluntary modulation. Each trial lasted 50 s, including 5 s at the start and end of each trial without perturbation. The second task was a time-invariant condition, without bias force, where participants were instructed to keep their wrist relaxed while angular perturbations were applied. For both tasks, the same perturbation signal was used as during the simulation study

with the rotation of the wrist restricted to 0.02 rad and excited frequencies between 0.1-19.3 Hz (section IV.D – Fig. 5a).

D. Data Analysis

The same data preprocessing was performed as for the simulation study: part of the data was discarded and the remaining data was decimated.

The exerted time-varying voluntary torque was applied to ensure time-varying joint properties, but is not relevant for the estimator. Therefore, before performing system identification, the 0.05 Hz time-varying voluntary exerted torque was removed by fitting and subtracting a low-frequency signal composed of a constant, a linear function and four goniometric functions $(\cos(\omega t), \sin(\omega t), \cos(2\omega t), \sin(2\omega t))$ (Figure 5b – white solid line).

For the skirt decomposition and KBR method the same model structure and parameters were used as during the simulation study. The order of the time variation for the skirt method was set to $N_p = 7$ and the hyperparameter σ for the KBR method was set to ~20s, with γ based on the variance of the data.

Quality of the estimators

The quality of the estimators was assessed using the VAF (17). Next to the VAF on the data set used for the estimation, each estimator of a single trial was validated on the five other trials within a participant. Before determining the VAF, frequencies below 0.8 Hz were removed as these frequencies are dominated by trial-to-trial variability in voluntary motor control and have little contribution to joint dynamics.

E. Comparison with other techniques

The two proposed identification methods for joint impedance were compared with two other methods previously presented. Both methods are ensemble averaging methods, requiring multiple repetitions of the same time-varying behaviour. The first is a method proposed by Ludvig and Perreault [45] who used a non-parametric estimator in time domain to successfully identify joint impedance averaging across short data segments (SDS) and multiple (but a reduced number of) realizations [27]. We implemented this method ourselves. The second method is one designed by Guarin and Kearney [40] (scripts available online) who combine ensemble and deterministic approaches to estimate TV joint impedance.

For a fair comparison of the methods, those presented in this paper and those by Guarin and Ludvig five of the six collected trials are used as an input for estimating the joint impedance model and the sixth trial is used for validation. For the SDS method we used a window length of 100 samples, i.e. this is the time window over which joint impedance is considered time-invariant, and a maximum lag of the impulse response function of 40 ms.

Fig. 5 approximately here

F. Results

Position and torque data are presented in Fig. 5b. The position data is equivalent to the imposed perturbation. Torque data shows the torque exerted by the participant, expressed as a percentage of their maximum voluntary torque level, on top of the rapid torque changes as resulting from the applied position perturbation.

Skirt decomposition method

Fig. 6 presents the results obtained when using the skirt decomposition method on the experimental data. The measured and fitted output spectrum are well matched at, and close to, the excited frequencies (Fig. 6a). The green dashed line gives the estimated noise floor.

The corresponding system function shows a sinusoidally varying joint stiffness and resonance frequency analogue to the sinusoidal exerted voluntary torque (Fig. 6b). This is highlighted in its 2D representation (Fig. 6c - top left). Fig. 6c shows the system function of all six trials recorded for this participant. All trials demonstrate a sinusoidal-like change in joint stiffness and resonance frequency, however with marked inter-trial variability. All together, VAF_{self} for the non-parametric skirt decomposition method for all trials and all participants was on average 84.3% ± 4.6% (mean ± *SD*) (range for individual participants: 66-91%) (Table II). The estimated model for joint impedance estimated on a single trial was validated on the other five trials. On average this resulted in a VAF_{val} of 66.1 ± 6.0 % (mean ± *SD*) (range for individual participants: 40-83%).

Analysis of the task without bias force, i.e. no time-variying behaviour, confirmed time-invariant joint dynamics with a similar resonance frequency across the full time window. Moreover, VAF_{self} and VAF_{val} were >93% for all trials of all participants.

Table II approximately here

Fig. 6 approximately here

KBR identification

Fig. 7 presents the results obtained when using KBR identification with the recorded data. The frozen FRF (Fig. 7a) demonstrates a sinusoidally varying joint stiffness and resonance frequency, for all trials performed by this participant (Fig. 7b). The VAF_{self} for the parametric KBR identification method on the trials performed by the first participant was on average 76.4% ± 7.3% (mean ± SD) (range for individual participants: 52-90%) (Table II). The estimated model for joint impedance estimated on a single trial was validated on the other five trials. On average this resulted in a VAF_{val} of 75.8 ± 7.3 % (mean ± *SD*) (range for individual participants: 51-89%).

Analysis of the task without bias force, i.e. no time-variying behaviour, confirmed time-invariant joint dynamics with a similar resonance frequency across the full time window. Moreover, VAF_{self} and VAF_{val} were >97% for all trials of all participants.

Fig. 7 approximately here

Comparison with other techniques

Table II presents the VAF for all participants when ensemble data was used of five trials for estimating the joint impedance model, and the sixth trial was used for validation. In addition

to the KBR and skirt method, results are presented for the SDS and Guarin method. On average, the KBR method provides the best results (VAF_{val} = 76.8 ± 7.2 %) closely followed by the skirt method (VAF_{val} = 75.3 ± 5.4 %). The other methods perform similar but on average have a lower VAF (SDS: VAF_{val} = 61.6 ± 7.2 %; Guarin: VAF_{val} = 63.1 ± 7.2 %).

VI. Discussion

In this section, results from the simulation and experimental study will be discussed in light of the new identification procedures to quantify joint impedance.

A. Parametric and non-parametric identification of joint impedance

This study demonstrates that it is possible to obtain a good model fit based on a single trial of data, in line with some other recent studies [35, 36]. Both the KBR method and skirt decomposition method revealed a sinusoidal time-varying resonance frequency and joint stiffness. The time-varying system dynamics of the human wrist resembled the time-varying simulated joint stiffness or instructed joint torque. Both algorithms require little a priori information about the expected time variations. The minimal information provided to the estimator about time-varying behavior contrasts the commonly employed linear parameter varying (LPV) models. LPV models require a measured time-dependent scheduling function that induce the change of the model parameters [35, 46]. There are no assumptions about the order of the system dynamics, or a scheduling variable, in the skirt decomposition method, but it assumes the time variations can be described by a set of smooth basis functions. For the KBR method, the order of system dynamics is set a priori and the hyperparameter σ determines the smoothness of the time variation.

The performance of the KBR method depends on the choice of the model order and on the values for the hyperparameters σ and γ. Although a 2nd-order joint impedance model has been used often in the literature, in this study a 3rd-order model (3 zeros, 2 poles) was used. The choice for a 3rd-order model structure was made based the joint dynamics (modelled as a 2nd-order mass-spring-damper system) and the grip dynamics to capture the interaction between the joint and the manipulator [1]. A 3rd-order model may better capture the musculoskeletal structure for joints where multiple muscles act around a joint (agonist-antagonist muscle pairs) [47]. Fixed values were used for the hyperparameters in the presence of noise. Lataire, et al. [39] developed an optimisation procedure to determine the optimal values for the hyperparameters by minimizing a leave-two-out-cross validation criterion (LTO-CV) [48]. However, this criterion proved to be fairly insensitive to the value of the hyperparameters, as soon as they are in an acceptable range. Hyperparameter σ was chosen in accordance with our expectations; $\sigma \approx 20s$, which is of the same order of magnitude as the period of the exerted time variation. This value ensures that the resulting estimate is smooth, effectively suppressing noise contributions. The hyperparameter γ was chosen near the global minima of the LTO-CV evaluated for all the trials, as our results were insensitive to the exact value of γ.

The non-parametric skirt decomposition method does not require an a priori defined model order and thereby has more flexibility to capture the dynamics, albeit smooth, as dictated by the used basis functions. The method needs a multisine perturbation signal that includes sufficient excited frequencies to quantify the system dynamics and at the same time leaves appropriate space between excited frequencies to capture the time variations in the skirts. When measuring humans, the frequency resolution is limited as the measurement time in humans is restricted e.g. to prevent fatigue. This is critical at the lowest frequencies up to ~5 Hz, where the human has the ability to modulate his/her joint impedance. Hence, up to 5 Hz ideally there are many excited frequencies that allow proper identification of joint impedance but at the same time sufficient unexcited frequencies are required to capture time-varying behavior. The non-parametric nature of the skirt method provides more freedom at the cost of a greater variance especially below the resonance frequency.

For both methods a well-defined LTV model could be constructed using only a single trial of 30 s of data (VAF_{val} > 70%). Up to ~90% of the data could be explained using either the KBR method or the skirt based method (on the estimation data set). An explanation for the high VAFs (>85%) in some and low VAFs (< 70%) in others may be found in the sensitivity of the methods to the smoothness of the time variation, i.e. data sets from participants that were better at smoothly following a sinusoidally time-varying torque resulted in higher VAFs. The skirt method suffers less of this as no a priori model structure is applied. However, the lower VAFs on validation data compared to estimation data (drop by ~10-20%), not seen for the KBR method, may indicate overfitting. It is noteworthy that validation based on single trial data may not only reflect modelling errors but will also be negatively affected due to inherent human trial-to-trial variability. This is reflected in the results of the trials without bias force, i.e. participants are fully relaxed, which result in a higher VAF as the human does not intervene. Moreover, the trials without bias force demonstrate the methods do not have any a priori assumptions on time variance, provided they fit time invariant data well.

A potential limitation of the methods is the speed of time variation that can be successfully identified. The 0.05 Hz time-varying torque that was used is slower than most relevant time-varying human behavior (~1-2 Hz for e.g. human walking). Preliminary simulations have demonstrated that the KBR method can identify these rapid time-variations by optimizing its hyperparameters. However, this will result in a model of higher complexity, and therefore higher uncertainty as there is a greater risk of modelling noise. The skirt decomposition method is unable to capture rapid time-variations using the current design of the multisine perturbation signal. It will require optimization of the multisine perturbation signal to provide greater space between excited frequencies. Considering the limited bandwidth of human joints this may become difficult. Future work will have to establish the exact possibilities and constraints of both methods for identifying time-varying joint impedance.

In the present study the comparison with ensemble based methods of Ludvig and Perreault [4] and Guarin and Kearney

[40] revealed consistently higher VAFs on a validation trial for the KBR and skirt method. However, both methods were developed with a pseudorandom arbitrary level perturbation signal, which is different from a multisine as applied in this study.. Therefore the only conclusions to draw from the comparison is that the KBR and skirt method allow a better estimate of a model for joint impedance based on limited data collected using a multisine perturbation and under slowly time-varying behavior.

B. Time-varying human joint impedance

Observing a time-varying joint stiffness and resonance frequency when varying the level of torque is in line with earlier reports [7, 9, 49]. An increasing resonance frequency, accompanied with an increase in joint stiffness, was reported for the ankle joint when generating a torque by pushing the foot down (i.e. plantarflexion) [9]. The KBR method demonstrates a similar sinusoidal pattern in joint stiffness. Impedance is high when torque is high, and vice versa. For the skirt method, this distinction is less clear. This may be partly attributed to the frequency resolution inherent to the non-parametric skirt method.

The KBR method (Fig. 7b) also reveals a change in the size of the peak at the resonance frequency. This peak is larger for higher levels of torque which may be attributed to the underlying mechanisms that allow humans to successfully complete the requested motor task. Humans can adapt the mechanical behavior of their joints by regulating intrinsic and reflexive joint properties [1, 50]. Intrinsic properties can be tuned by co-contracting, activating different muscles that act in opposite directions around a joint at the same time, effectively resulting in an increased joint impedance. This is primarily expressed in a change in intrinsic stiffness, which has a greater sensitivity for muscle activation than intrinsic viscosity [7, 49]. Reflexive properties cannot be voluntarily adjusted and depend on pre-programmed stimulus-response characteristics of the nervous system. Whereas intrinsic properties are primarily tuned feedforward, reflex properties involve feedback pathways with an inherent time delay. An increase in torque level up to 20% MVT has been demonstrated to raise the contribution of both the intrinsic and reflexive stiffness [7, 35]. A larger reflexive contribution will result in enhanced oscillatory behavior at the resonance frequency as the reflexive (feedback) pathway involves a time delay resulting in phase lags [51]. This may explain the increased resonance peaks when the generated torque increases to 20% MVT. The currently employed identification technique does not yet allow for separation of intrinsic and reflexive contributions to the motor behavior but this is worked on. This could for example be done by fitting a parametric model to the TV-FRFs so to extract these detailed parameters that determine joint impedance [1].

VII. General Conclusion

This study presents a novel framework for the identification of time-varying joint impedance by making use of two different LTV SI methods. Both the parametric kernel-based regression (KBR) method and the non-parametric skirt method allow identification of joint impedance over time using a single trial of data. Despite the low SNR of the recorded signals in the biomedical domain, there is the possibility to successfully quantify changes in joint impedance over time based on limited data. In future this may allow to gain valuable new insights in how humans control their limbs and learn new tasks. The successful application of SI methods unknown in the biomedical domain demonstrates that cross domain collaborations are important to make full use of all that the field of system identification has to offer in studying human control behavior.

VIII. Appendix

A. Skirt decomposition method

This appendix summarizes the algorithm for the skirt decomposition method, which is proposed in [37]. The model in (7) is approximated in a frequency band comprising three successive excited frequencies, denoted k_{e}^{-}, k_{e} and k_{e}^{+}, as

$$Y_m(k) \approx \frac{1}{N}\sum_{p=0}^{N_{\mathrm{p}}} \sum_{k'\in\{k_{\mathrm{e}}^{-},k_{\mathrm{e}},k_{\mathrm{e}}^{+}\}} G_p(j\omega_{k'})U(k') \ldots B_p(k-k') + I_Y(j\omega_k) \tag{A.1}$$

expressed in the frequencies $k = k_e^{-} - \Delta_{k_e}, \ldots, k_e^{+} + \Delta_{k_e}$ with

$$I_Y(k) = \sum_{n=0}^{N_{\mathrm{r}}} r_n\, k^n \tag{A.2}$$

a polynomial in k, which captures $T_Y(j\omega_k)$ and the fact that only a limited number of terms from (7) are included in (A.1), $\Delta_{k_{\mathrm{e}}}$ is the distance (in bins(between two excited frequencies. By solving (A.1) for $G_p(j\omega_{k'})$ and r_n in least squares sense, for all $k_e \in \mathbb{K}_{exc}$, the LTI blocks G_p are effectively estimated non-parametrically (i.e. at the excited frequencies only) in a sliding frequency band. Note that (A.1) is linear in all the unknowns ($G_p(j\omega_{k'})$ and r_n).

B. Kernel based regression method

This appendix summarizes the algorithm for the KBR method, which is proposed in [39]. The estimate is defined as

$$\hat{a}_n, \hat{b}_n = \underset{a_n, b_n}{\operatorname{argmin}} \sum_{k\in\mathbb{K}_{\mathrm{int}}} \frac{|E(k,a_n,b_n)|^2}{\hat{\sigma}_E^2(k,a_n,b_n)} \ldots + \sum_{n=1}^{N_a} \breve{a}_n^T K^{-1} \breve{a}_n + \sum_{n=0}^{N_b} \breve{b}_n^T K^{-1} \breve{b}_n \tag{B.1}$$

With

$$E(k,a_n,b_n) = DFT\left\{ y - \sum_{n=0}^{N_b} b_n u^{(n)} + \sum_{n=1}^{N_a} a_n y^{(n)} \right\}_k \tag{B.2}$$

$$a_n = \mathring{a}_n + \breve{a}_n, \quad b_n = \mathring{b}_n + \breve{b}_n$$

where a_n and b_n are vectorised versions of $a_n(t)$ and $b_n(t)$ in $t = 0, T_s, \ldots, (N-1)T_s$, $u^{(n)}$ and $y^{(n)}$ are the sampled and vectorised nth derivatives of $u(t)$ and $y(t)$. The parameters a_n and b_n are decomposed into $\mathring{a}_n$ and $\mathring{b}_n$ (which are constant

vectors to which no regularisation is applied) and $\breve{a}_n$ and $\breve{b}_n$ (which are time-varying and regularised to impose their smoothness). The latter is done by including the sums of $\breve{a}_n^T K^{-1} \breve{a}_n$ and $\breve{b}_n^T K^{-1} \breve{b}_n$. The kernel matrix K is semi-positive definite and symmetric, and imposes structure on the estimated parameters.

σ_E^2 is the variance of E. Explicit expressions for E and σ_E^2, based on the sampled signals $u(t)$ and $y(t)$ are available in[39].

Note that (B.2) is a non-quadratic (and in general non-convex) problem, due to the division by $\hat{\sigma}_E^2$. This is solved via an iterative convex relaxation, where $\hat{\sigma}_E^2$ is initialized to 1 and, for the mth iteration, is computed as $\hat{\sigma}_{E,m}^2(k) \leftarrow \hat{\sigma}_E^2(k, \hat{a}_{n,m-1}, \hat{b}_{n,m-1})$, with $\hat{a}_{n,m-1}, \hat{b}_{n,m-1}$ the estimates obtained at the $(m-1)^{\text{th}}$ iteration. This algorithm is outlined in Section 6.2 of [39]. The computation of $\hat{\sigma}_E^2$ also requires an estimate of the noise variance on the measured spectra, which is computed via the method presented in [52].

Note that this estimator does not require the explicit computation of K^{-1}. This allows for the use of (close to) singular kernel matrices.

REFERENCES

[1] F. C. van der Helm, A. C. Schouten, E. de Vlugt, and G. G. Brouwn, "Identification of intrinsic and reflexive components of human arm dynamics during postural control," *J Neurosci Methods,* vol. 119, pp. 1-14, Sep 15 2002.

[2] E. Todorov, "Optimality principles in sensorimotor control," *Nat Neurosci,* vol. 7, pp. 907-15, Sep 2004.

[3] E. J. Perreault, R. F. Kirsch, and P. E. Crago, "Multijoint dynamics and postural stability of the human arm," *Exp Brain Res,* vol. 157, pp. 507-17, Aug 2004.

[4] D. Ludvig and E. J. Perreault, "System identification of physiological systems using short data segments," *IEEE Trans Biomed Eng,* vol. 59, pp. 3541-9, Dec 2012.

[5] D. Ludvig, E. J. Perreault, and R. E. Kearney, "Efficient estimation of time-varying intrinsic and reflex stiffness," *Conf Proc IEEE Eng Med Biol Soc,* vol. 2011, pp. 4124-7, 2011.

[6] D. Ludvig, I. Cathers, and R. E. Kearney, "Voluntary modulation of human stretch reflexes," *Exp Brain Res,* vol. 183, pp. 201-13, Nov 2007.

[7] M. M. Mirbagheri, H. Barbeau, and R. E. Kearney, "Intrinsic and reflex contributions to human ankle stiffness: variation with activation level and position," *Exp Brain Res,* vol. 135, pp. 423-36, Dec 2000.

[8] R. E. Kearney and I. W. Hunter, "Dynamics of human ankle stiffness: variation with displacement amplitude," *J Biomech,* vol. 15, pp. 753-6, 1982.

[9] I. W. Hunter and R. E. Kearney, "Dynamics of human ankle stiffness: variation with mean ankle torque," *J Biomech,* vol. 15, pp. 747-52, 1982.

[10] R. M. Enoka and J. Duchateau, "Muscle fatigue: what, why and how it influences muscle function," *J Physiol,* vol. 586, pp. 11-23, Jan 01 2008.

[11] Y. Van Ingelgem, E. Tourwé, J. Vereecken, and A. Hubin, "Application of multisine impedance spectroscopy, FE-AES and FE-SEM to study the early stages of copper corrosion," *Electrochimica Acta,* vol. 53, pp. 7523-7530, 2008/10/30/ 2008.

[12] G. F. Sirca and H. Adeli, "System identification in structural engineering," *Scientia Iranica,* vol. 19, pp. 1355-1364, 2012/12/01/ 2012.

[13] M. D. Spiridonakos and S. D. Fassois, "Parametric identification of a time-varying structure based on vector vibration response measurements," *Mechanical Systems and Signal Processing,* vol. 23, pp. 2029-2048, 2009/08/01/ 2009.

[14] J. Ertveldt, J. Lataire, R. Pintelon, and S. Vanlanduit, "Frequency-domain identification of time-varying systems for analysis and prediction of aeroelastic flutter," *Mechanical Systems and Signal Processing,* vol. 47, pp. 225-242, 2014/08/03/ 2014.

[15] J. Lataire and R. Pintelon, "Frequency-domain weighted non-linear least-squares estimation of continuous-time, time-varying systems," *IET Control Theory & Applications,* vol. 5, pp. 923-933, 2011.

[16] P. Z. Csurcsia and J. Lataire, "Nonparametric Estimation of Time-Varying Systems Using 2-D Regularization," *IEEE Transactions on Instrumentation and Measurement,* vol. 65, pp. 1259-1270, 2016.

[17] R. Zou and K. H. Chon, "Robust algorithm for estimation of time-varying transfer functions," *IEEE Trans Biomed Eng,* vol. 51, pp. 219-28, Feb 2004.

[18] J. K. Hammond and P. R. White, "The analysis of non-stationary signals using time-frequency methods," *Journal of Sound and Vibration,* vol. 190, pp. 419-447, 1996/02/29/ 1996.

[19] W. J. Staszewski and D. M. Wallace, "Wavelet-based Frequency Response Function for time-variant systems - An exploratory study," *Mechanical Systems and Signal Processing,* vol. 47, pp. 35-49, 2014.

[20] S. Conforto and T. D'Alessio, "Spectral analysis for non-stationary signals from mechanical measurements: A parametric approach," *Mechanical Systems and Signal Processing,* vol. 13, pp. 395-411, 1999/05/01/ 1999.

[21] R. Pintelon and J. Schoukens, *System identification: a frequency domain approach*: John Wiley & Sons, 2012.

[22] E. Sobhani Tehrani, K. Jalaleddini, and R. E. Kearney, "Linear parameter varying identification of ankle joint intrinsic stiffness during imposed walking movements," *Conf Proc IEEE Eng Med Biol Soc,* vol. 2013, pp. 4923-7, 2013.

[23] R. B. Stein and R. E. Kearney, "Nonlinear behavior of muscle reflexes at the human ankle joint," *J Neurophysiol,* vol. 73, pp. 65-72, Jan 1995.

[24] R. F. Kirsch and R. E. Kearney, "Identification of time-varying stiffness dynamics of the human ankle joint during an imposed movement," *Exp Brain Res,* vol. 114, pp. 71-85, Mar 1997.

[25] D. J. Bennett, J. M. Hollerbach, Y. Xu, and I. W. Hunter, "Time-varying stiffness of human elbow joint during cyclic voluntary movement," *Exp Brain Res,* vol. 88, pp. 433-42, 1992.

[26] H. Lee and N. Hogan, "Time-Varying Ankle Mechanical Impedance During Human Locomotion," *IEEE Trans Neural Syst Rehabil Eng,* vol. 23, pp. 755-64, Sep 2015.

[27] D. Ludvig, M. Plocharski, P. Plocharski, and E. J. Perreault, "Mechanisms contributing to reduced knee stiffness during movement," *Exp Brain Res,* Jul 15 2017.

[28] D. Ludvig, T. S. Visser, H. Giesbrecht, and R. E. Kearney, "Identification of time-varying intrinsic and reflex joint stiffness," *IEEE Trans Biomed Eng,* vol. 58, pp. 1715-23, Jun 2011.

[29] J. B. MacNeil, R. E. Kearney, and I. W. Hunter, "Identification of time-varying biological systems from ensemble data," *IEEE Trans Biomed Eng,* vol. 39, pp. 1213-25, Dec 1992.

[30] J. F. Soechting, J. R. Dufresne, and F. Lacquaniti, "Time-varying properties of myotatic response in man during some simple motor tasks," *J Neurophysiol,* vol. 46, pp. 1226-43, Dec 1981.

[31] M. Mulder, T. Verspecht, D. A. Abbink, M. M. van Paassen, D. C. Balderas, A. Schouten*, et al.*, "Identification of Time Variant Neuromuscular Admittance using Wavelets," *2011 Ieee International Conference on Systems, Man, and Cybernetics (Smc),* pp. 1474-1480, 2011.

[32] M. P. Vlaar, T. Solis-Escalante, A. N. Vardy, F. C. T. van der Helm, and A. C. Schouten, "Quantifying Nonlinear Contributions to Cortical Responses Evoked by Continuous Wrist Manipulation," *IEEE Trans Neural Syst Rehabil Eng,* vol. 25, pp. 481-491, May 2017.

[33] C. M. Harris and D. M. Wolpert, "Signal-dependent noise determines motor planning," *Nature,* vol. 394, pp. 780-4, Aug 20 1998.

[34] S. H. Scott and G. E. Loeb, "The computation of position sense from spindles in mono- and multiarticular muscles," *J Neurosci,* vol. 14, pp. 7529-40, Dec 1994.

[35] M. A. Golkar, E. Sobhani Tehrani, and R. E. Kearney, "Linear Parameter Varying Identification of Dynamic Joint Stiffness

during Time-Varying Voluntary Contractions," *Front Comput Neurosci,* vol. 11, p. 35, 2017.

[36] D. L. Guarin and R. E. Kearney, "Time-varying identification of ankle dynamic joint stiffness during movement with constant muscle activation," *Conf Proc IEEE Eng Med Biol Soc,* vol. 2015, pp. 6740-3, 2015.

[37] J. Lataire, R. Pintelon, and E. Louarroudi, "Non-parametric estimate of the system function of a time-varying system," *Automatica,* vol. 48, pp. 666-672, Apr 2012.

[38] L. A. Zadeh, "Frequency Analysis of Variable Networks," *Proceedings of the IRE,* vol. 38, pp. 291-299, 1950.

[39] J. Lataire, R. Pintelon, D. Piga, and R. Toth, "Continuous-time linear time-varying system identification with a frequency-domain kernel-based estimator," *Iet Control Theory and Applications,* vol. 11, pp. 457-465, Feb 2017.

[40] D. L. Guarin and R. E. Kearney, "Estimation of Time-Varying, Intrinsic and Reflex Dynamic Joint Stiffness during Movement. Application to the Ankle Joint," *Front Comput Neurosci,* vol. 11, p. 51, 2017.

[41] A. C. Schouten, E. d. Vlught, and F. C. T. v. d. Helm, "Quantification of spinal reflexes in neurological disorders," in *2004 IEEE International Conference on Systems, Man and Cybernetics (IEEE Cat. No.04CH37583)*, 2004, pp. 2492-2499 vol.3.

[42] J. Lataire, E. Louarroudi, and R. Pintelon, "Detecting a time-varying behavior in frequency response function measurements," *IEEE Transactions on Instrumentation and Measurement,* vol. 61, pp. 2132-2143, 2012.

[43] R. Pintelon, E. Louarroudi, and J. Lataire, "Nonparametric time-variant frequency response function estimates using arbitrary excitations," *Automatica,* vol. 51, pp. 308-317, 2015/01/01/ 2015.

[44] A. C. Schouten, E. de Vlugt, J. J. van Hilten, and F. C. van der Helm, "Design of a torque-controlled manipulator to analyse the admittance of the wrist joint," *J Neurosci Methods,* vol. 154, pp. 134-41, Jun 30 2006.

[45] D. Ludvig and E. J. Perreault, "Estimation of joint impedance using short data segments," *Conf Proc IEEE Eng Med Biol Soc,* vol. 2011, pp. 4120-3, 2011.

[46] J.-W. van Wingerden and M. Verhaegen, "Subspace identification of Bilinear and LPV systems for open- and closed-loop data," *Automatica,* vol. 45, pp. 372-381, 2009/02/01/ 2009.

[47] E. Sobhani Tehrani, K. Jalaleddini, and R. E. Kearney, "Ankle Joint Intrinsic Dynamics is more Complex than a Mass-Spring-Damper Model," *IEEE Trans Neural Syst Rehabil Eng,* Mar 08 2017.

[48] J. Lataire, D. Piga, and R. Tóth, "Frequency-domain least-squares support vector machines to deal with correlated errors when identifying linear time-varying systems," *IFAC Proceedings Volumes,* vol. 47, pp. 10024-10029, // 2014.

[49] P. L. Weiss, I. W. Hunter, and R. E. Kearney, "Human ankle joint stiffness over the full range of muscle activation levels," *Journal of Biomechanics,* vol. 21, pp. 539-544, 1988/01/01/ 1988.

[50] T. R. Nichols and J. C. Houk, "Improvement in linearity and regulation of stiffness that results from actions of stretch reflex," *J Neurophysiol,* vol. 39, pp. 119-42, Jan 1976.

[51] A. C. Schouten, E. de Vlugt, J. J. van Hilten, and F. C. van der Helm, "Quantifying proprioceptive reflexes during position control of the human arm," *IEEE Trans Biomed Eng,* vol. 55, pp. 311-21, Jan 2008.

[52] J. Lataire and R. Pintelon, "Estimating a nonparametric colored-noise model for linear slowly time-varying systems," *IEEE Transactions on Instrumentation and Measurement,* vol. 58, pp. 1535-1545, 2009.

Mark van de Ruit received the M.Sc. degree in biomedical engineering from Delft University of Technology, the Netherlands, in 2011. He obtained the Ph.D degree in neurophysiology from the University of Birmingham, United Kingdom, in 2016.

He is currently a postdoctoral researcher at Delft University of Technology, the Netherlands. His research interest is in neuromuscular control, combing electrophysiological recording techniques with system identification to obtain a better understanding of human motion control in healthy individuals and those suffering of movement disorders.

Gaia Cavallo received the M.Sc. degree in Systems and Control and Biomedical Engineering (cum laude) both from Delft University of Technology, the Netherlands, in 2017.

She recently started a Ph.D. with the Department ELEC, Vrije Universiteit Brussel, Belgium. Her research interest is in system identification of biomedical applications.

John Lataire (S'06–M'11) was born in Brussels, Belgium, in 1983. He received the Electrical Engineer degree in electronics and information processing and the Ph.D. degree in engineering sciences (Doctor in de Ingenieurswetenschappen) from the Vrije Universiteit Brussel, Brussels, in 2006 and 2011, respectively. From October 2007 to October 2011, he was on a Ph.D. fellowship from the Research Foundation—Flanders (FWO). Since August 2006, he has been working as a Researcher with the Department ELEC-VUB, Brussels.

Dr. Lataire is the coauthor of more than 30 articles in refereed international journals. He received the 2008 IOP outstanding paper award (best paper in Measurement Science & Technology), the Best Junior Presentation Award 2010 at the 29th Benelux Meeting on Systems and Control, was the co-recipient of the 2014 Andy Chi award (best paper in IEEE Trans. on Instrumentation and Measurement), and was the recipient of the 2016 J. Barry Oakes Advancement Award (from the IEEE Instrumentation and Measurement society).

His main interests include the frequency domain formulation of the identification of dynamic systems, with a specific focus on the identification of time-varying systems, and the use of kernel-based regression in system identification.

Frans C. T. van der Helm received the M.Sc. degree in human movement science and the Ph.D. degree (cum laude) in mechanical engineering in 1985 and 1991, respectively. He is a Professor of Biomechatronics and Bio-Robotics with the Delft University of Technology, Delft, The Netherlands, and an Adjunct Professor with the University of Twente, Enschede, The Netherlands, and Northwestern University, Evanston, IL, USA.

He is one of the programme leaders in the Medical Delta, the NeuroSIPE Program, and H-Haptics Program. His current

research interests include biomechanics of the upper and lower extremity, neuromuscular control, eye biomechanics, pelvic floor biomechanics, human motion control, and posture stability.
Prof. van der Helm was a recipient of an ERC Advanced Grant on "4D EEG: A new tool to assess the spatial and temporal activity in the cortex."

Winfred Mugge received the MSc and PhD degrees in mechanical engineering from Delft University of Technology, the Netherlands, in 2006 and 2011, respectively. During his PhD research at the Biomechanical Engineering Department, he performed research on muscle force feedback and movement disorders within Trauma Related Neuronal Dysfunction (TREND) and NeuroSIPE, Dutch multidisciplinary research consortia. From 2013 to 2015 he was a postdoctoral researcher at VU University Amsterdam and since then he has been working as an assistant professor at Delft University of Technology. His research interest is in human motor control, neuromechanics, haptics, system identification and orthotics.

Jan-Willem van Wingerden was born in Ridderkerk, The Netherlands, in 1980. He received the B.S. and Ph.D. (cum laude) degrees from the Delft Center for Systems and Control, Delft University of Technology, The Netherlands, in 2004 and 2008, respectively. His Ph.D. thesis was entitled Smart Dynamic Rotor Control for Large Offshore Wind Turbines. He was with Philips Applied Technologies, Eindhoven, The Netherlands. He is currently a Professor with the Delft University of Technology, Delft, Netherlands. His current research interests include linear parameter varying identification, subspace identification, smart structures and control, and identification of wind turbines and wind farms.

Alfred C. Schouten received the M.Sc. and Ph.D. degrees in mechanical engineering from Delft University of Technology, Delft, The Netherlands, in 1999 and 2004, respectively. He is currently an Associate Professor at Delft University of Technology and the University of Twente, Enschede, The Netherlands. He is a Co-Founder of the Delft Laboratory for Neuromuscular Control. His research interests include the field of neuromuscular control and techniques to quantify the functional contribution of afferent feedback, neuromuscular modeling, haptic manipulators, and system identification. His research focuses on both able-bodied individuals and individuals suffering from movement disorders.

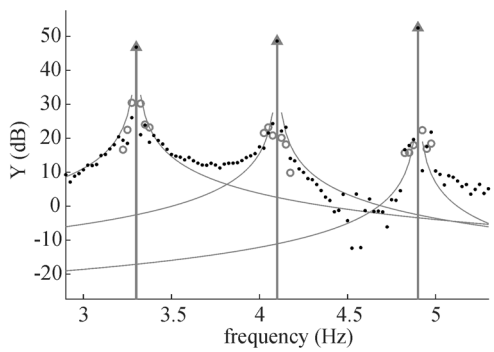

Fig. 1 The black dots give the output spectrum of a time-varying system, excited by a sparse multisine. This output spectrum is decomposed into: 1) excited frequencies (vertical arrows), 2) skirt shaped contributions (grey full lines), and 3) discrete spectral contributions (grey circles) which are due to the periodic nature of the applied time variation.

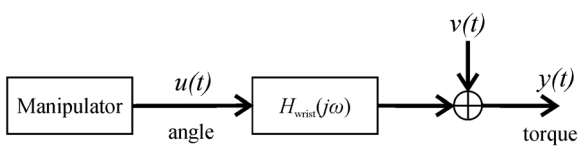

Fig. 2 The system of the human wrist. The manipulator provides a multisine position input ($\boldsymbol{u(t)}$) to the human wrist of which the dynamics are represented by $\boldsymbol{H(j\omega)}$. The measured torque output $\boldsymbol{y(t)}$ is assumed to contain measurement noise $\boldsymbol{v(t)}$.

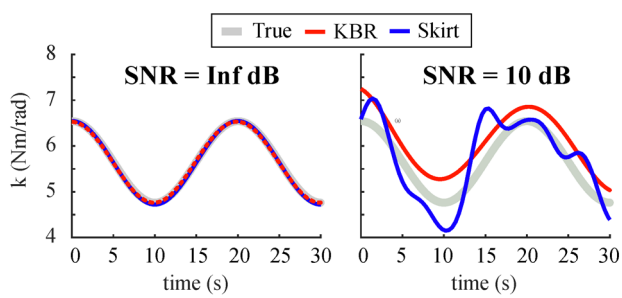

Fig. 3 Joint impedance estimates obtained using the KBR and skirt method from simulation data. Simulations were ran including a time-varying joint impedance both without (SNR = Inf dB) and with (SNR = 10 dB) output noise. Both the KBR and skirt method allow to obtain a good estimate of joint impedance despite the presence of output noise.

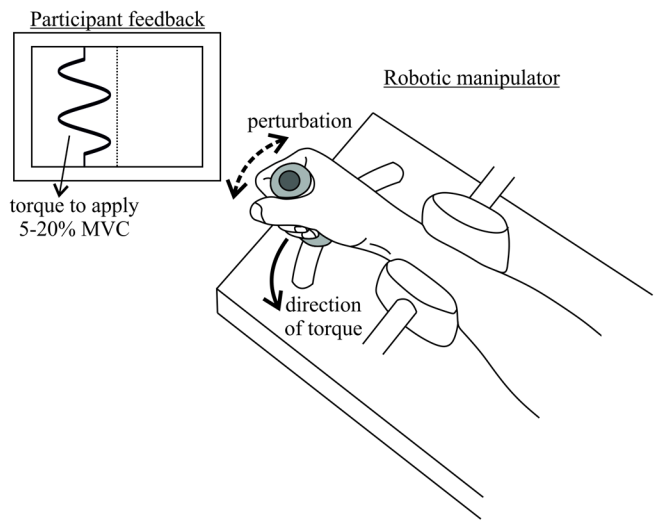

Fig. 4 Experimental setup used to measure time-varying joint impedance. The right arm of the participant was fixated, with the flexion-extension axis of the wrist aligned with the axis of rotation of the handle of the manipulator. Multisine position perturbations were imposed on the handle while the participant had to track a sinusoidal torque pattern. Feedback on torque exerted and target torque level was provided on a monitor directly in front of the participant.

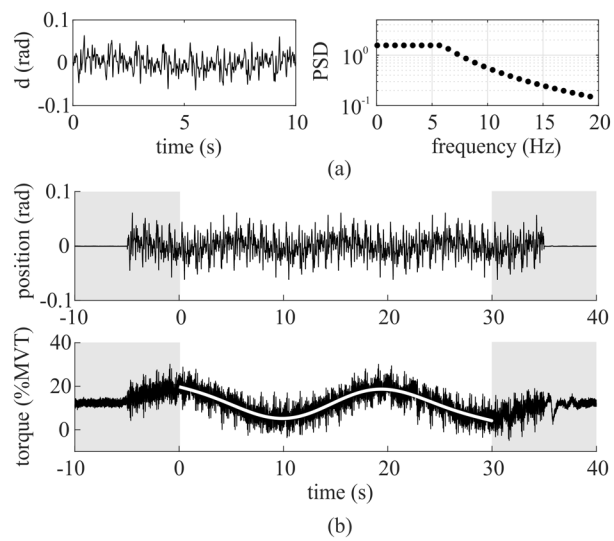

Fig. 5 Details of perturbation signal and raw data recorded. (a) Position perturbation signal in frequency and time domain. Perturbation signal is built of 10 s periods, containing only frequencies between 0.1-19.3 Hz ($\Delta f = 0.8$ Hz). (b) Raw position and torque data recorded during a single trial. The shaded areas are data not analyzed to avoid modelling artefacts or transient effects. The voluntary exerted sinusoidal time-varying torque (white line) was removed prior to analysis, as it only served to obtain time-varying joint impedance.

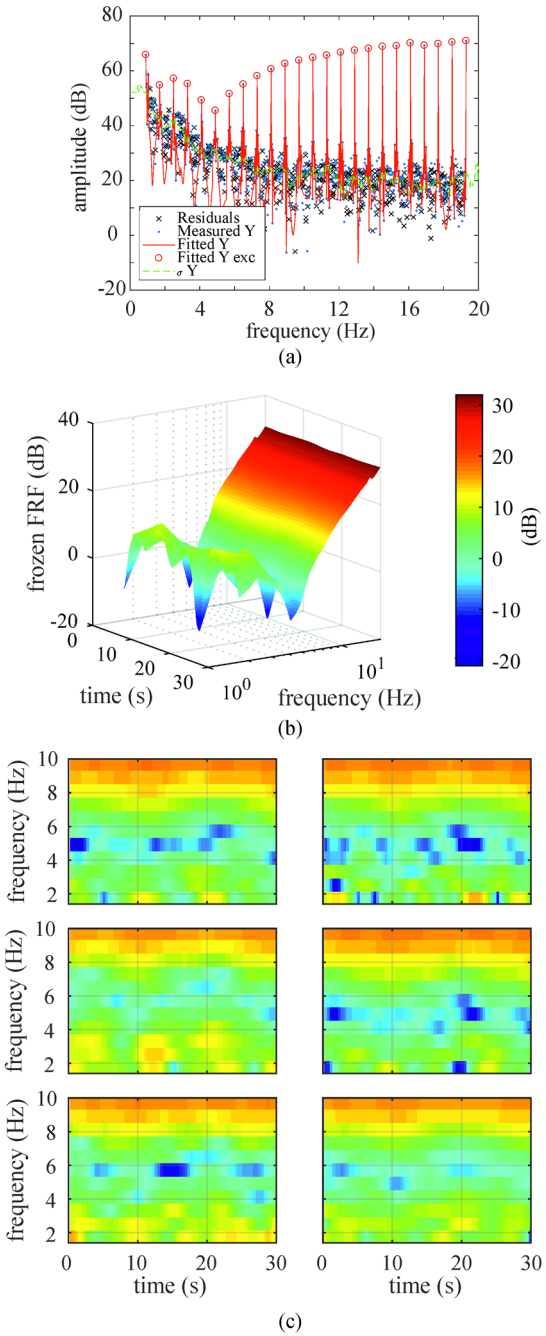

Fig. 6 Results obtained using the skirt decomposition method. (a) Measured (dots) output spectrum, fitted (red line) output spectrum and their difference (residuals – crosses). The green line indicates the noise floor. (b) Estimated system function, as defined in (2) with the estimated $\boldsymbol{G_p}$. (c) System function for all trials recorded for a single participant in the condition where voluntary torque was sinusoidally varied between 5-20% of maximum voluntary torque. Color scale same as in (b).

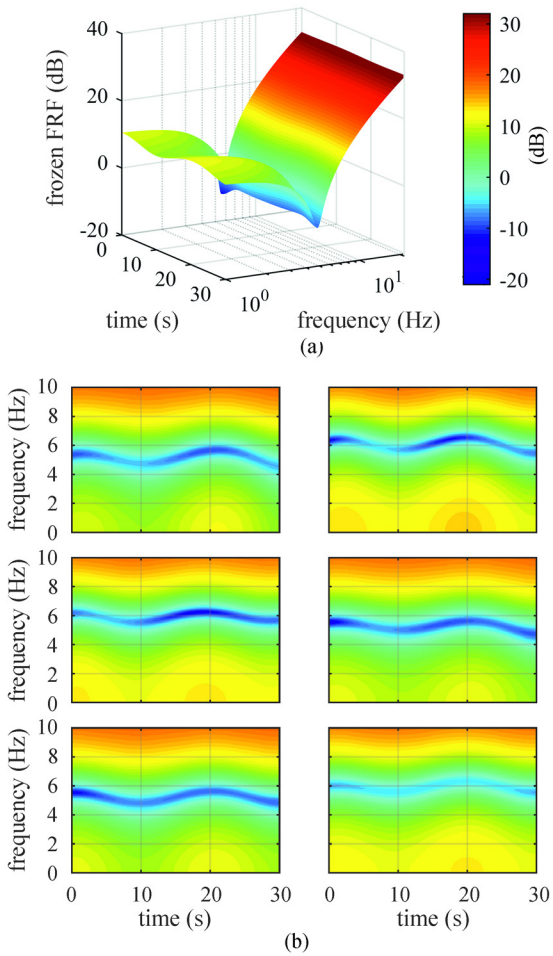

Fig. 7 Results obtained using the kernel based method. (a) Estimated frozen FRF, using kernel-based regression. (b) Frozen FRF for all trials recorded in a single participant in the condition where voluntary torque was sinusoidally varied between 5-20% of maximum voluntary torque. Color scale same as in (a).

TABLE I
VAFS FOR SIMULATION DATA

	VAF_{self} [%] 10 dB	**VAF_{val} [%] Inf dB**	**VAF_{val} [%] 10 dB**
KBR	96.7	99.9	96.7
Skirt	97.7	98.2	94.9

Variance-Accounted-For (VAF) for both KBR and skirt method when using simulation data with and without noise. The model estimate is based on a single trial with 10dB filtered white noise and validated on de data used for estimation (left column). In addition, validation is performed on a trial without noise (Inf dB – middle column) and trial with different noise realization (right column).

TABLE II
VAFS FOR EXPERIMENTAL DATA

	Single trial				**Ensemble**			
	KBR		**Skirt**		**KBR**	**Skirt**	**SDS**	**Guarin**
	VAF_{self} [%] mean±S.D.	VAF_{val} [%] mean±S.D	VAF_{self} [%] mean±S.D	VAF_{val} [%] mean±S.D	VAF_{val} [%] mean±S.D	VAF_{val} [%] mean±S.D	VAF_{val} [%] mean±S.D	VAF_{val} [%] mean±S.D
P1	89,7±3.0	89.1 ± 2.9	91.2 ± 3.3	82.9 ± 3.3	89.2± 2.9	87.3± 3.2	60.6± 3.4	61.6± 2.5
P2	88.8 ± 5.0	88.1 ± 4.5	90.8 ± 3.9	81.8 ± 3.9	88.6± 4.8	86.5± 3.8	80.1± 5.7	81.4± 6.2
P3	80.8 ± 8.7	79.9 ± 9.0	85.5 ± 7.3	76.2 ± 6.9	80.6± 8.6	80.0± 5.1	71.3± 9.8	73.3± 10.5
P4	52.4 ± 14.5	51.4 ± 14.2	66.1 ± 8.0	39.8 ± 9.3	52.4± 14.5	51.8± 9.4	40.8± 12.0	43.6± 11.9
P5	75.8 ± 5.2	75.4 ± 5.5	86.3 ± 3.1	66.7 ± 7.2	75.8± 5.2	74.7± 7.3	61.9± 6.4	62.8± 6.7
P6	70.9 ± 7.4	71.3 ± 7.4	85.8 ± 2.2	60.6 ± 4.8	71.1± 7.5	71.6± 3.5	54.6± 5.9	56.1± 5.5
Overall	**76.4 ± 7.3**	**75.8 ± 7.3**	**84.3 ± 4.6**	**66.1 ± 6.0**	**76.3 ± 7.2**	**75.3 ± 5.4**	**61.6 ± 7.2**	**63.1 ± 7.2**

Variance-Accounted-For (VAF) for both KBR and skirt method when using experimental data. The left side shows VAFs for each participant when estimates were based on a single trial of data. Mean ± S.D. of 6 VAFs is shown when validation is performed on the data used for estimation (VAF_{self}), and 30 VAFs when the one trial is used for estimation and the other five for validation (VAF_{val}),. The right side of the table shows VAFs for four different methods (KBR, Skirt decomposition, Short Data Segments (SDS) and Guarin) when the ensemble average of 5 trials was used for model estimation and the sixth trial for validation (e.g. Mean ± S.D. of 36 VAFs).